Radiología 66 (2024) S65–S74

RADIOLOGÍA

www.elsevier.es/rx

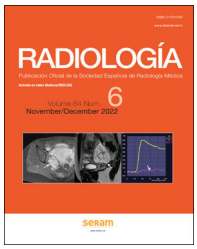

UPDATE AND GOOD PRACTICE IN THE CONTRAST MEDIA USES

Ways of analysing extracellular gadolinium enhancement

C. Casillas Meléndez

Servicio de Diagnóstico por Imagen, Consorcio Hospitalario Provincial de Castellón, Castellón, Spain

Received 26 February 2024; accepted 3 April 2024
Available online 12 November 2024

KEYWORDS
Image interpretation;
Multiparametric magnetic resonance imaging;
Contrast media;
Perfusion imaging;
Radiomics;
Artificial intelligence

Abstract The use of extracellular gadolinium-based contrast agents provides valuable information in magnetic resonance studies, thus increasing diagnostic confidence. These contrast agents make it easier to detect and define injuries, and narrow down the differential diagnosis. They are indicated for several different reasons, both for diagnostic purposes and for evaluating the response to treatment. Morphological analysis can assess the type of uptake, the qualitative and semiquantitative study of the signal intensity vs time curves in multiphase sequences, and the quantitative analysis of the uptake with T1 or T2* perfusion studies associated with pharmacokinetic models.

Multiphase dynamic studies with 3D sequences contain valuable information that is not exploited by a simple visual analysis of 2D images. To take advantage of this information and the imaging biomarkers provided, computational analysis should be used. To this end, the future role of artificial intelligence is increasingly evident.

PALABRAS CLAVE
Interpretación de imagen;
Resonancia magnética muliparamétrica;
Medio de contraste;
Imagen de perfusión;
Radiómica;
Inteligencia artificial

Tipos de análisis de la captación de Gadolinio extracelular

Resumen El uso de agentes de contraste extracelular basados en Gadolinio proporciona información valiosa en los estudios de RM, aumentando la confianza diagnóstica. Amplifican la capacidad para detectar y delimitar lesiones, así como para acotar el diagnóstico diferencial. Sus indicaciones son múltiples, tanto para el diagnóstico como para la evaluación de la respuesta al tratamiento. Su estimación puede realizarse con el análisis morfológico del tipo de captación, el estudio cualitativo y semicuantitativo de las curvas de intensidad de señal vs tiempo en secuencias multifase, o analizando cuantitativamente la captación con estudios de perfusión T1 o T2* asociados a modelos farmacocinéticos.

E-mail address: casillasmel@gmail.com

2173-5107/

Los estudios dinámicos multifase con secuencias 3D contienen información valiosa que no se utiliza con el simple análisis visual de las imágenes 2D. Para aprovechar esta información subyacente, que proporciona biomarcadores de imagen, es necesario el análisis computacional. En este aspecto, el futuro papel de la Inteligencia Artificial se hace cada día más evidente.

Introduction

Gadolinium-based contrast agents (GBCAs) are extremely safe and widely used in clinical practice. The European Medicines Agency prohibited the use of the high-risk agents that cause nephrogenic systemic fibrosis, which has resulted in the near total disappearance of this delayed-onset complication. Both the retention of gadolinium (Gd) in different organs and the environmental impact caused by its presence in waste water mean that it must be used with care, and the risks and benefits should be assessed on a case-by-case basis.[1]

GBCAs help detect and demarcate lesions that are hard to identify on non-contrast sequences, enabling precise measurement and assessment of adjacent structure involvement. GBCAs are not limited to the study of tumours; they can also be used to assess pathologies that are inflammatory (for example, Crohn's disease through Magnetic Resonance (MR) Enterography,[2] infectious (for example, spondylodiscitis)[3] or vascular (MR angiography).[4] The enhancement of focal lesions in solid organs makes it easier to narrow the differential diagnosis because their biodistribution and behaviour in dynamic sequences allow lesions to be clustered into groups. Furthermore, these agents enable us to assess tumour response to pharmacological and radiotherapeutic treatment. Therefore, GBCAs play a vital role throughout the diagnostic and follow-up process, especially in cancer patients.[5]

There are different ways of assessing the contrast uptake of lesions: morphological, qualitative, semi-quantitative and quantitative. On the one hand, the morphology of the uptake or signal intensity vs. time (SI/T) curves can be assessed in multiphasic studies with T1-weighted sequences.[6] On the other hand, quantitative analysis can be performed using pharmacokinetic models in both T1-weighted sequences (based on GBCAs at low concentrations)[7] and T2*-weighted images (exploiting the magnetic susceptibility of these agents at high concentrations).[8]

It is relatively straightforward to assess the biodistribution of contrast or the morphology of SI/T curves when using 2D multiphase sequences. By contrast, if we wish to perform a volumetric analysis over time—before, during and after the contrast agent administration—the vast amount of data necessitates the use of computational calculations. The extracted information provides imaging biomarkers, which will form part of the patient's diagnostic and prognostic assessment.[9] Similarly, artificial intelligence (AI) can be trained on this extensive dataset so that lesions can be detected and characterised more easily.[10]

The aim of this article is to outline the different analytical techniques that can be used to evaluate MR images acquired after GBCA administration.

Morphological analysis

GBCAs produce an increase in SI due to their ability to shorten the longitudinal relaxation time (T1) at low concentrations. T1-weighted sequences (spin echo [SE] or gradient echo [GE]) are used to identify this SI enhancement.[11]

The acquisition of T1-weighted sequences prior to contrast administration enables the increase in SI following contrast administration to be assessed by comparing the two sequences. Nevertheless, interpretation can sometimes still be complex despite the pre-contrast acquisition, specifically in lesions that are hyperintense in T1. It is difficult to assess the increase of SI in lesions that have high SI in T1 before intravenous contrast administration. Applying subtraction to the two sequences eliminates the areas with no uptake, making it easier to identify the areas with uptake[12] (Fig. 1). However, the subtraction technique is limited by the patient moving between the two sequences as this causes a spatial misalignment of pixels. Subtraction images are especially useful in MR angiography studies, which make it easier to visualise distal vessels in maximum intensity projections. Likewise, in lesions with a haemorrhagic component, subtraction can suppress it and differentiate between haemorrhagic areas and areas with contrast uptake.

Similarly, there have been reports of a paradoxical signal decrease in hyperintense focal hepatic lesions after GBCA administration, so pre-administration baseline imaging is helpful in their interpretation.[13]

The use of spectral fat suppression in T1-weighted SE sequences facilitates the detection of contrast agent uptake. Its use is particularly indicated for the assessment of soft tissue tumours.

Morphological analysis on static 2D images acquired after contrast agent administration is a first step to more accurately delineating lesions. The morphology of the uptake can be homogeneous, heterogeneous, nodular or linear. Areas with no contrast uptake within the lesions represent necrotic areas. Increased SI in structures adjacent to focal lesions can be a helpful associated finding in narrowing the differential diagnosis, even if it is non-specific. For example, in the central nervous system (CNS), dural enhancement in an extra-axial location adjacent to a lesion

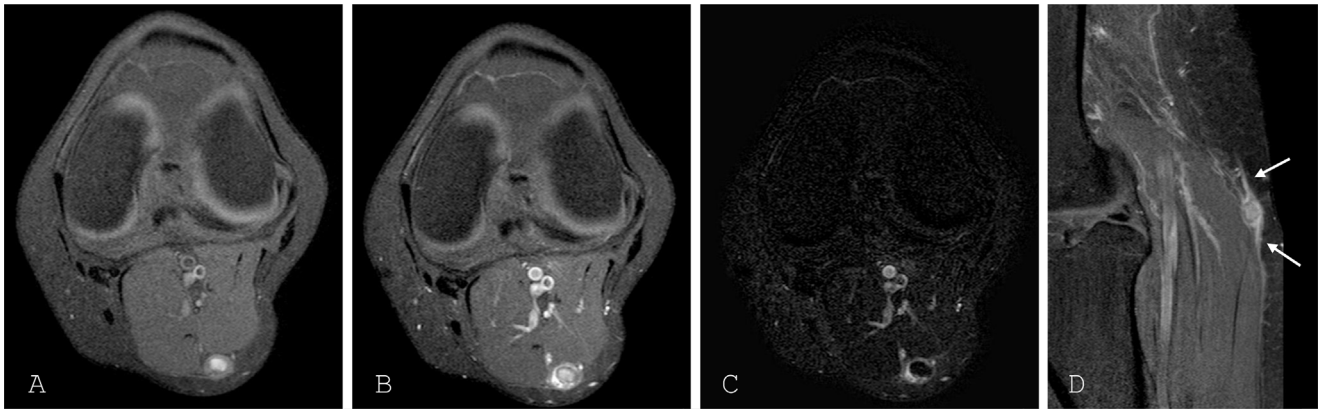

Figure 1 Use of non-GBCA-enhanced sequence. A) T1-weighted transverse image with spectral fat suppression. A soft tissue lesion is seen in the posterior region of the knee, with a hyperintense centre. B) T1-weighted image with spectral fat suppression after GBCA administration. C) Synthetic image obtained by subtraction (B − A), identifying peripheral contrast uptake, without enhancement in the centre of the lesion. D) Sagittal T1-weighted image after GBCA administration. Linear contrast enhancement adjacent to the lesion (arrows). AP: schwannoma of the sural cutaneous nerve.

Figure 2 T1-weighted spin echo transversal image after GBCA administration. Extra-axial lesion with intense homogeneous increase in signal intensity and thickening and contrast enhancement in the adjacent dura mater (arrows). Meningioma.

Figure 3 Transverse spin-echo T1-weighted image after GBCA administration. Uptake with linear morphology located in the cerebral sulci (arrows). Leptomeningeal carcinomatosis.

with marked contrast uptake is virtually diagnostic of meningioma (Fig. 2). Likewise, the uptake of a nerve in contiguity with an intensely enhancing soft tissue tumour narrows the differential diagnosis to a lesion of neural origin, such as schwannoma (Fig. 1D). Linear uptake in the topography of the cerebral sulci in cancer patients with clinical onset in several cranial nerves is highly suspicious for leptomeningeal metastases (Fig. 3). The morphology and location of delayed contrast uptake in cardiac MRI studies is critical. Subendocardial enhancements in defined coronary territories reflect the presence of fibrosis in chronic infarction. Mesoventricular or epicardial uptake enables the diagnosis of other entities such as hypertrophic cardiomyopathy, myocarditis or sarcoidosis.[14]

Static studies with SE or GE sequences have limitations in post-treatment assessment. Chemotherapy, radiother-

Table 1 Multiphase dynamic sequence. Temporal resolution depending on the organ under study.

Organ	Temporal resolution of each phase	Total acquisition time
Prostate	10 s	4 min
Breast	60 s	5–7 min
Heart	100–125 ms	40–50 beats
Osteomuscular	6 s	4 min
CNS	3–6 s	3–5 min

apy, target drugs and immunotherapy alter the tumour microenvironment, impacting vascular tumour neoformation, inflammatory processes and the immune response. All this will influence contrast uptake, given that it will lead to decreased vascularisation, hypoxia and increased vascular permeability.[15] For example, contrast uptake in a CNS astrocytoma treated with antiangiogenic agents and radiotherapy might indicate post-treatment changes, pseudo-progression or tumour progression.[16] For these cases we must use other types of analysis.

Qualitative analysis

Dynamic multiphase sequences are used to analyse the characteristics of the contrast distribution in the lesions. This is achieved using T1-weighted 2D or 3D GE sequences with or without spectral fat suppression. The same sequence is repeated in the same location before, during and after IV administration of the GBCA.

The dose of contrast agent is 0.1 mmol/kg body weight, administered with an infusion pump at a rate of 2–3 ml/s. Next, 20 ml of saline solution should be administered at the same rate to ensure that any remaining contrast is injected and also to compact the contrast bolus. The length of the multiphase dynamic sequence, or temporal resolution, varies depending on the organ under study.[17–21] Considerable variability exists between the sequence used, depending on the brand of MRI scanner, as well as between different organs and indications. Table 1 shows the most commonly used characteristics according to the organ under study.

The morphology of contrast uptake during the dynamic sequence (biodistribution) is crucial for lesion characterisation, for example in liver tumours. Although there is overlap between the different lesions and their behaviour in dynamic studies, in most cases it provides information that aids in lesion characterisation. For example, a liver tumour with nodular and peripheral contrast uptake in the early phases, which progresses towards the centre of the lesion and is hyperintense with respect to the surrounding liver in the last phase of the dynamic sequence is typically a haemangioma (Fig. 4). Hepatic hypervascular lesions show intense uptake in the arterial phase, with contrast washout in the other phases of the dynamic sequence. This contrast biodistribution can be identified in focal nodular hyperplasia (Fig. 5), certain subtypes of adenoma, in hepatocellular nodules in the cirrhotic liver, and in hypervascular metastases.

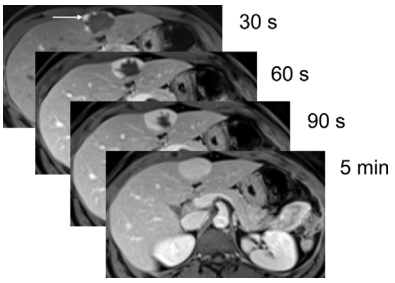

Figure 4 Dynamic multiphase T1-weighted gradient echo sequence with spectral fat suppression after GBCA administration. Hepatic haemangioma with nodular and peripheral contrast uptake in the initial phases of the dynamic study (white arrow), progressing towards the centre during the sequence. In the last phase, it is completely filled with contrast, being hyperintense with respect to the adjacent liver parenchyma.

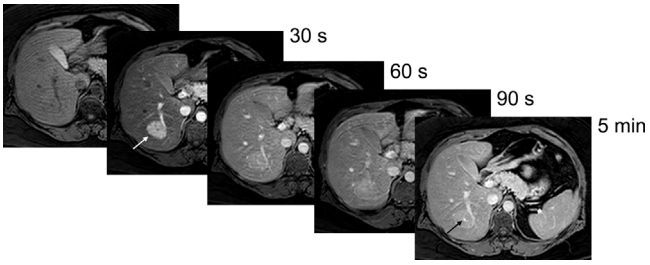

Figure 5 Dynamic multiphase T1-weighted gradient echo sequence with spectral fat suppression. Focal lesion in segment VII of the liver, isointense in the non-contrast phase, with hypervascular behaviour: intense enhancement in the arterial phase (white arrow), with progressive washout. There is a small central scar with slow and progressive contrast uptake (black arrow). Focal nodular hyperplasia.

The development of free breathing sequences (4D dynamics) is a major breakthrough in the study of liver dynamics. These are fast GE 3D T1-weighted sequences with spectral fat suppression,[22] which have a two-fold advantage: they considerably reduce respiratory artifacts and have a high temporal resolution (<3 s per phase). This improved temporal resolution allows the definition of variable times for multiple phases. Thus, the temporal resolution can be increased in the early phases to obtain several arterial times while the temporal resolution can be decreased and the spatial resolution increased in the later phases of the dynamic study (Fig. 6).[23]

Signal intensity vs. time curves

Defining a region of interest (ROI) in an organ or lesion in a dynamic sequence enables the graphical representation of SI variation over time. A qualitative assessment of these curves facilitates lesion characterisation.[6] The morphology of the SI/T curve allows the lesions to be divided into groups; the different types of curves are illustrated in Fig. 7. Most benign lesions (prostate or breast, for example) show a slowly progressive or type 2 curve. In contrast, most malignant lesions present arterial-type curves, with a rapid and intense increase in SI and a progressive decrease in the rest

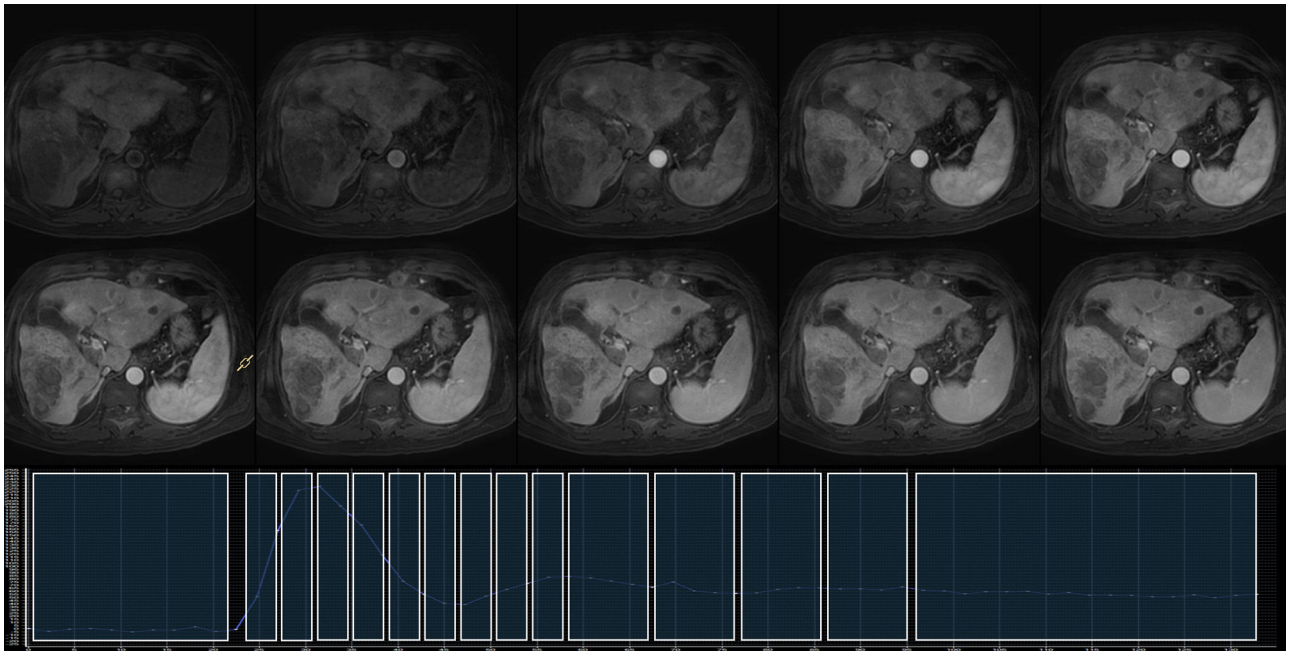

Figure 6 Dynamic sequence with free breathing (dynamic 4D). Improved temporal resolution with variable times for multiple phases. Higher temporal resolution in the early phases with several arterial times and predominance of spatial resolution in the later phases of the dynamic study. Multicentre hepatocarcinoma. Courtesy of Gerard Blasco Sola (Philips Ibérica S.A.).

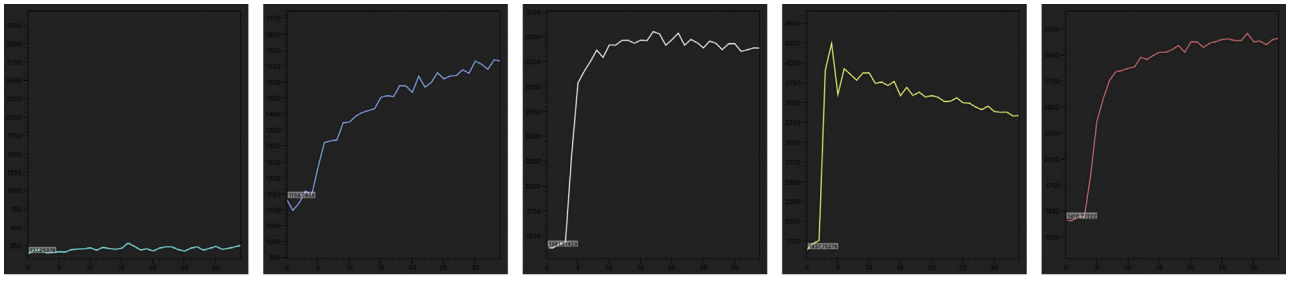

Figure 7 Qualitative analysis with SI/T curves. Type 1 curve: no enhancement (cysts, benign lesions). Type 2 curve: slow progressive enhancement (benign lesions). Type 3 curve: intense and early enhancement with persistent SI (indeterminate lesions). Type 4 curve: intense and early enhancement with a progressive decrease of SI (malignant lesions). Type 5 curve: intense, early and progressive enhancement (inflammatory lesions).

of the dynamic study (type 4). Inflammatory lesions undergo early and intense uptake, progressing through the remainder of the study (type 5). Lesions with an intense and early increase in their SI, which is maintained during the dynamic sequence (type 3) are indeterminate and can be seen in benign or malignant lesions.[24,25] Absence of contrast uptake (type 1 curves) indicates benign lesions. However, it should be noted that there is some overlap between the different types of curves. SI/T curves are not routinely obtained, but they are still very useful for assessing response to treatment, for example in neoadjuvant breast cancer or musculoskeletal tumours. Dynamic studies and assessment of SI/T curves facilitate the identification and assessment of prostate MRI findings using the PI-RADS score, although the current trend is to use reduced protocols (biparametric studies) without administering GBCAs.

Unlike CT, where the concentration of iodinated contrast is proportional to the attenuation of the x-rays (HU), in MRI the concentration of Gd cannot be derived directly from the SI, unless pharmacokinetic models are used. In semi-quantitative analyses, SI/T curves can be assessed using a number of parameters, such as time to peak (TTP), area under the curve at 60% (AUC60), peak enhancement, brevity of enhancement, time to maximum slope or wash-in and wash-out rate. Malignant lesions often show a hypervascular curve, with short TTP, increased AUC60 and pronounced wash-in. These descriptors can be coded using a colour scale and superimposed on a morphological image to obtain a parametric map that facilitates the identification of specific lesions according to their behaviours (Fig. 8).

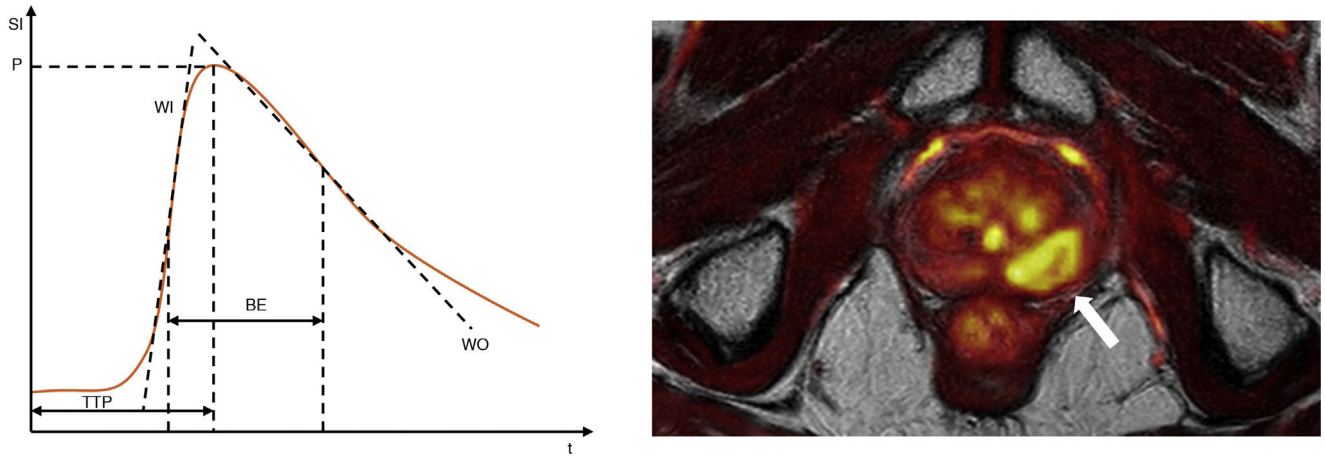

Figure 8 SI/T curve descriptors and parametric image. BE: brevity of enhancement; time between the point of maximum absorption and maximum disappearance; P: Peak, maximum contrast SI; TTP: time to peak; WI: wash-in or absorption rate; WO: wash-out rate. Colour-coded wash-in map, identifying a focal lesion in the left posterior-medial region of the peripheral zone of the prostate corresponding with clinically significant cancer (arrow).

Quantitative analysis

GBCAs have an effect on both longitudinal (T1) and transverse (T2) relaxation times. This effect is predominantly concentration-dependent. At low concentrations, T1 shortening predominates, with an increase in SI in T1-weighted sequences, and at high concentrations, T2 shortening predominates, with a decrease in SI in T2-weighted sequences.[26] T1 and T2 perfusion sequences are based on this physical property.

T1 perfusion studies

T1 perfusion sequences are based on the relaxivity of the GBCAs, in other words, on the ability to shorten T1. They are mainly used in oncology, for example, to assess breast and prostate tumours.

Quantitative analysis with T1 perfusion studies uses compartmental pharmacokinetic models. The model most commonly used is the Tofts model, which differentiates between the vascular space and the extravascular-extracellular space.[27] The movement of substances between these two compartments can be quantified with different constants; the most common being K^{trans} (transfer from the intravascular to the extravascular space), K_{ep} (return from the extracellular interstitium to the vascular space), V_e (extravascular-extracellular space fraction) and V_p (plasma volume fraction). They provide non-invasive physiological information by studying the first passage of contrast through the capillary network and rapid diffusion into the extravascular-extracellular space. They can also quantify capillary permeability and assess both the return of contrast to the intravascular space and its elimination.

For this purpose, it is necessary to calculate the native T1 relaxation times (prior to contrast administration) with two GE sequences with different flip angles, as well as the arterial input function by means of an ROI in an artery included in the study area. The most commonly used perfusion sequences are volumetric fast GE sequences with spectral fat suppression. They should have a time resolution of 4–10 s, with a total acquisition time of between 3 and 6 min; for the calculation of the K^{trans} constant, the time should not be less than 3 min and for Vp, Ve and Kep not less than 6 min. A standard dose of Gd (0.1 mmol/kg) is used at a rate of 2–3 ml/s, followed by 25 ml of saline at the same rate.

Quantitative studies with T1 perfusion include lesion characterisation, prognostic assessment, treatment planning, assessment of response to treatment and detection of neoplastic recurrence (Fig. 9).

T2* perfusion studies

These are based on the magnetic susceptibility of Gd at high concentrations, which leads to a decrease in the SI of the tissues. They reflect capillary tissue perfusion and blood volume.[28]

Echo planar imaging sequences are used for acquisition, with a time resolution of 1.5–2 s per dynamic phase, and a total acquisition time of less than 2 min. Although results improve with high doses of Gd (0.2 mmol/kg), standard concentrations (0.1 mmol/kg) are commonly used. In contrast to T1 perfusion studies, the speed of administration (5 ml/s) must be increased in magnetic susceptibility studies to compact the contrast bolus and encourage a high concentration in the bloodstream. This is followed by 25 ml of saline which is administered at the same rate. To reduce the inherent effect of Gd on T1 time, a low dose of Gd (2–3 ml) can be administered a few minutes before the T2* perfusion study is performed.[29]

These analyses are used in cerebral vascular accidents for tumour characterisation, in prognostic stratification and in the assessment of response to chemotherapy or radiotherapy. Relative cerebral blood volume (rCBV) has been proposed as an imaging biomarker for the prediction of survival in high-grade gliomas.[30]

These studies provide non-invasive in vivo insights into the microvascular environment by quantifying different

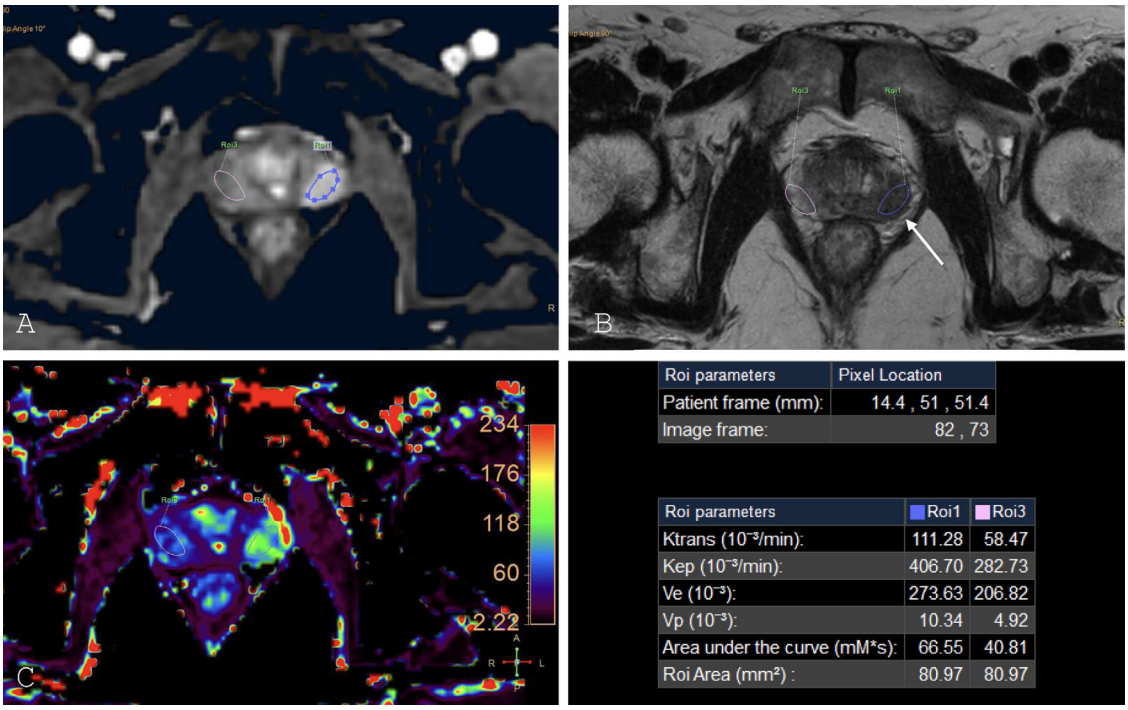

Figure 9 T1 perfusion. A) Image of the dynamic sequence with GBCA with ROI in the peripheral prostate zone. B) Axial T2-weighted TSE image with suspicious finding in the left posterior-lateral region of the peripheral zone of the prostate (arrow). C) Parametric map with K^{trans} values using a bicompartmental pharmacokinetic model. The table shows elevated K^{trans} and K_{ep} values in the suspicious area corresponding to clinically significant prostate cancer (PI-RADS 5).

parameters: rCBV, cerebral blood flow (rCBF), time to peak (TTP), mean transit time (MTT) and percentage of SI recovery (PSR).[30]

Table 2 summarises the biological properties that can be analysed with MR perfusion studies, the parameters that are assessed and their correlations.

The results of the quantitative analysis based on the T1 and T2* perfusion studies are strongly influenced by the technical parameters used in the pulse sequences (repetition time, echo time, flip angle), the contrast volume, the injection rate and the relaxivity of GBCAs. This variability makes it difficult to compare the data obtained, not only between different hospitals, but also in progress studies performed in the same radiology department, whether using the same MRI equipment or not. To reduce this variability as far as possible, one proposal is to standardise the entire process, including MRI sequence parameters, the post-processing methods used and the generation of data. The software used for the assessment of perfusion studies should follow the recommendations of expert consensus and adapt to rapid developments.[31]

Imaging biomarkers, computational analysis and artificial intelligence

An imaging biomarker is a characteristic that is extracted from images of a subject, which can be objectively measured using computational techniques and which behaves as an indicator of a normal biological process, disease or response to a therapeutic intervention.[32] Radiomics is based on the multivariate analysis of large numbers of imaging biomarkers extracted from the processing of radiological images with the aim of finding a relationship with a diagnosis, prognosis or therapeutic efficacy.[33]

Dynamic MRI sequences with GBCAs and perfusion studies provide a wealth of data that can be analysed computationally. In clinical practice we usually evaluate 2D images over time, following contrast agent administration. The ideal strategy would be to be able to analyse a complete 3D volume over time during the dynamic sequence, for example in breast, brain or prostate pathology. The magnitude of data in these cases means the application of data reduction techniques is essential, through which highly correlated variables are eliminated. Classification algorithms are also applied, to statistically analyse whether the patient population can be distributed according to the imaging characteristics.

A volumetric study with dynamic breast MRI, acquiring 192 slices with a resolution of 512×512 pixels, generates approximately 50 million SI/T curves. Computational analysis is used to segment the different types of curves found, reduce their dimensionality and homogenise them in order to reduce the effect of patient movement during the different phases, or the variability of time from the start of the sequence to the injection of the contrast agent. Iterative clustering algorithms, such as K-means, succeed in reducing the set of SI/T curves. Subsequently, alignment algorithms are used between the time sequences (dynamic time warping), in search of similarities between the SI/T curves, thus minimising transit times (contrast agent injection time) and distortion (different temporal resolution), detecting

Table 2 Quantitative analysis with MRI perfusion studies. Biological properties, parameters and correlation.

MRIPerfusion	Biological properties	Quantitative parameters	Correlation
T1	Percentage of uptake of GBCA in tissues Assessment of the vascular and extravascular spaces	Initial Gd area under the curve K^{trans} and K_{ep}: transfer constants between vascular and extravascular space, return to vascular space from extracellular interstitium Ve: extracellular extravascular space fraction Vp: plasma volume fraction	Density of vessels Vascular permeability Perfusion Plasma volume
T2*	Effects of GBCA on the magnetic field Depends on blood volume and flow Assesses the vascular space	rBV: relative blood volume rBF: relative blood flow MTT: mean transit time Vessel size index	Vascular density Blood flow Temporal parameter Tumour grade

Figure 10 Application of AI in breast pathology. 3D image obtained from a dynamic volumetric sequence. AI differentiates between types of SI/T curves, grouping them together and colour-coding them in the space. Courtesy of Ángel Alberich-Bayarri (Quibim SL).

similar shapes, even if the series are out of phase or deformed.[34]

Artificial intelligence software can be trained with all this data to learn how to distinguish between the different patterns of SI/T curves and how they correlate with different types of injuries. After it is trained, AI can differentiate between different types of curves in a dynamic 3D volume, grouping them into benign, suspicious and malignant lesions, and locating them anatomically (Fig. 10).

Conclusions

The use of GBCAs in MRI is essential in a large number of diagnostic processes, whether they involve inflammatory, infectious or tumour pathology. They improve the ability of MRI to detect and delineate lesions, increasing diagnostic confidence. An evaluation of changes in MR images after contrast agent administration can be performed simply with morphological analysis in static studies or using

dynamic sequences. The SI/T curves obtained with dynamic multiphase sequences enable a qualitative analysis of the type of curve and a semi-quantitative analysis with the different descriptors. The application of pharmacokinetic models to dynamic sequences provides quantitative data and biomarkers for the differential diagnosis of lesions and the assessment of response to treatment. Computational analysis of the large amount of data obtained with dynamic 3D sequences and AI training will increase diagnostic accuracy and efficiency.

Funding

This research has not received funding support from public sector agencies, the business sector or any non-profit organisations.

Conflicts of interest

The authors declare that they have no conflicts of interest.

Acknowledgments

I would like to thank Ángel Alberich-Bayarri and the Quibim S.L. for providing comments, data and images as contribution to the section on biomarkers and artificial intelligence. Likewise, I would like to thank Gerard Blasco Sola and the Philips Ibérica S.A. for the material provided on the 4D free breathing sequences.

References

1. Barentsz JO, Richenberg J, Clements R, Choyke P, Verma S, Villeirs G, et al. ESUR prostate MR guidelines 2012. Eur Radiol. 2012;22:746–57.
2. Rimola J, Rodriguez S, García-Bosch O, Ordás I, Ayala E, Aceituno M, et al. Magnetic resonance for assessment of disease activity and severity in ileocolonic Crohn's disease. Gut. 2010;58:1113–20, http://dx.doi.org/10.1016/s0739-5930(09)79398-5.
3. Sadato N, Numaguchi Y, Rigamonti D, Kodama T, Nussbaum E, Sato S, et al. Spinal epidural abscess with gadolinium-enhanced MRI: serial follow-up studies and clinical correlations. Neuroradiology. 1994;36:44–8, http://dx.doi.org/10.1007/bf00599195.
4. Nagpal P, Grist TM. MR angiography contrast-enhanced acquisition techniques. Magn Reson Imaging Clin North Am. 2023;31:493–501, http://dx.doi.org/10.1016/j.mric.2023.04.007.
5. García-Figueiras R, Baleato-González S, Pahdani AR, Luna-Alcalá A, Vallejo-Casas JA, Sala E, et al. How clinical imaging can assess cancer biology. Insights Imaging. 2019;10:28, http://dx.doi.org/10.1186/s13244-019-0703-0.
6. Matsuda M, Takaharu T, Rui E, Wataru T, Shiori T, Kanako O, et al. Enhanced masses on contrast-enhanced breast: differentiation using a combination of dynamic contrast-enhanced MRI and quantitative evaluation with synthetic MRI. J Magn Reson Imaging. 2021;53:381–91, http://dx.doi.org/10.1002/jmri.27362.
7. Reynolds HM, Tadimalla S, Wang YF, Montazerolghaem M, Sun Y, Williams S, et al. Semi-quantitative and quantitative dynamic contrast-enhanced (DCE) MRI parameters as prostate cancer imaging biomarkers for biologically targeted radiation therapy. Cancer Imaging. 2022;22:71, http://dx.doi.org/10.1186/s40644-022-00508-9.
8. Shiroishi MS, Castellazzi G, Boxerman JL, D'Amore F, Essig M, Nguyen TB, et al. Principles of T2*-weighted dynamic susceptibility contrast MRI technique in brain tumor imaging. J Magn Reson Imaging. 2015;41:296–313, http://dx.doi.org/10.1002/jmri.24648.
9. European Society of Radiology (ESR). ESR statement on the validation of imaging biomarkers. Insights Imaging. 2020;11:76, http://dx.doi.org/10.1186/s13244-020-00872-9.
10. Marti-Bonmati L, Cerdá-Alberich L, Pérez-Girbés A, Díaz Beveridge R, Montalvá Orón E, Pérez Rojas J, et al. Pancreatic cancer, radiomics and artificial intelligence. Br J Radiol. 2022;95:72, http://dx.doi.org/10.1259/bjr.20220072.
11. Mitsumori LM, Bhargava P, Essig M, Maki JH. Magnetic resonance imaging using gadolinium-based contrast agents. Top Magn Reson Imaging. 2014;23:51–69, http://dx.doi.org/10.1097/rmr.0b013e31829c4686.
12. Lee VS, Flyer MA, Weinreb JC, Krinsky GA, Rofsky NM. Image subtraction in gadolinium-enhanced MR imaging. Am J Roentgenol. 1996;167:1427–32, http://dx.doi.org/10.2214/ajr.167.6.8956572.
13. Martí-Bonmatí L, Peñalosa F, Pastor MR, Villarreal E, Martínez MJ. Disminución paradójica de la señal tras administrar contraste en las lesiones hepaticas hiperintensas en resonancia magnética: un criterio de hemorragia intratumoral. Radiología. 2005;47:253–6, http://dx.doi.org/10.1016/s0033-8338(05)72844-7.
14. Pattanayak P, Bleumke DA. Tissue characterization of the myocardium state of the art characterization by magnetic resonance and computed tomography imaging. Radiol Clin North Am. 2015;53:413–23, http://dx.doi.org/10.1016/j.rcl.2014.11.005.
15. García-Figueiras R, Baleato-González S, Luna A, Muñoz- Iglesias J, Oleaga L, Vallejo Casas JA, et al. Assessing immunotherapy with functional and molecular imaging and radiomics. RadioGraphics. 2020;40:1987–2010, http://dx.doi.org/10.1148/rg.2020200070.
16. Brandes AA, Tosoni A, Spagnolli F, Frezza G, Leonardi M, Calbucci F, et al. Disease progression or pseudoprogression after concomitant radiochemotherapy treatment: pitfalls in neurooncology. Neuro Oncol. 2008;10:361–7, http://dx.doi.org/10.1215/15228517-2008-008.
17. Essig M, Shiroishi MS, Nguyen TB, Saake M, Provenzale JM, Enterline D, et al. Perfusion MRI: the five most frequently asked technical questions. Am J Roentgenol. 2013;200:24–34, http://dx.doi.org/10.2214/ajr.12.9543.
18. Kuhl CK, Mielcareck P, Klaschik S, Leutner C, Wardelmann E, Gieseke J, et al. Dynamic breast mr imaging: are signal intensity time course data useful for differential diagnosis of enhancing lesions? Radiology. 1999;211:101–10, http://dx.doi.org/10.1148/radiology.211.1.r99ap38101.
19. Kramer CM, Barkhausen J, Flamm SD, Kim RJ, Nagel E. Standardized cardiovascular magnetic resonance (CMR) protocols 2013 update. J Cardiovasc Magn Reson. 2013;15:91, http://dx.doi.org/10.1186/1532-429x-15-91.
20. Lin X, Lee M, Buck O, Woo KM, Zhang Z, Hatzogloy V, et al. Diagnostic accuracy of T1-weighted dynamic contrast-enhanced–MRI and DWI-ADC for differentiation of glioblastoma and primary CNS lymphoma. AM J Neuroradiol. 2015;53:345–53, http://dx.doi.org/10.3174/ajnr.a5023.
21. Tian Y, Adluru G. Dynamic contrast-enhanced MRI: basic physics, ulse sequences, and modeling. Adv Magn Reson Technol. 2020;1:321–44, http://dx.doi.org/10.1016/b978-0-12-817057-1.00015-9.
22. Reiner CS, Neville AM, Nazeer HK, Breault S, Dale BM, Merkle EM, et al. Contrast-enhanced free-breathing 3D T1-weighted gradient-echo sequence for hepatobiliary MRI in patients

with breath-holding difficulties. Eur Radiol. 2013;23:3087–93, http://dx.doi.org/10.1007/s00330-013-2910-2.
23. Park SH, Yoon JH, Park JY, Shim YS, Lee SM, Choi SJ, et al. Performance of free-breathing dynamic T1-weighted sequences in patients at risk of developing motion artifacts undergoing gadoxetic acid–enhanced liver MRI. Eur Radiol. 2023;33:4378–88, http://dx.doi.org/10.1007/s00330-022-09336-85:39 pm.
24. Verma S, Turkbey B, Muradyan N, Rajesh A, Cornud F, Haider MA, et al. Overview of dynamic contrast-enhanced MRI in prostate cancer diagnosis and management. Am J Roentgenol. 2012;198:1277–88, http://dx.doi.org/10.2214/ajr.12.8510.
25. El Khouli RH, Macura KJ, Jacobs MA, Khallil TH, Kamel IR, Dwyer A, et al. Dynamic contrast-enhanced MRI of the breast: quantitative method for kinetic curve type assessment. Am J Roentgenol. 2009;93:W295–300, http://dx.doi.org/10.2214/ajr.09.2483.
26. Rohrer M, Bauer H, Mintorovitch J, Requardt M, Weinmann HJ. Comparison of magnetic properties of MRI contrast media solutions at different magnetic field strengths. Investig Radiol. 2005;40:715–24, http://dx.doi.org/10.1097/01.rli.0000184756.66360.d3.
27. Sanz Requena R, Marti-Bonmati L, Álvarez C, García G, Pellicer A, Albercih-Bayarri A, et al. Resonancia magnética en la respuesta al tratamiento del síndrome de hiperestimulación ovárica: comparación de modelos farmacocinéticos. Radiología. 2009;51:176–82, http://dx.doi.org/10.1016/j.rx.2008.03.001.
28. Guzmán-de-Villoria JA, Fernández-García P, Mateos-Pérez JM, Desco M. Estudio de la perfusión cerebral mediante técnicas de susceptibilidad magnética: técnica y aplicaciones. Radiología. 2012;54:208–20, http://dx.doi.org/10.1016/j.rx.2011.06.003.
29. Boxerman JL, Quaarles CC, Hu LS, Erickson BJ, Gerstner ER, Smits M, et al. Consensus recommendations for a dynamic susceptibility contrast MRI protocol for use in high-grade gliomas. Neuro Oncol. 2020;22:1262–75, http://dx.doi.org/10.1093/neuonc/noaa141.
30. Lemasson B, Chenevert TL, Lawrence TS, Tsien C, Sundgren PC, Meyer CR, et al. Impact of perfusion map analysis on early survival prediction accuracy in glioma patients. Transl Oncol. 2013;6:766–74, http://dx.doi.org/10.1593/tlo.13670.
31. Pons-Escoda A, Smits M. Dynamic-susceptibility-contrast perfusion-weighted-imaging (DSC-PWI) in brain tumors: a brief up-to-date overview for clinical neuroradiologists. Eur Radiol. 2023;33:8026–30, http://dx.doi.org/10.1007/s00330-023-09729-3.
32. European Society of Radiology (ESR). White paper on imaging biomarkers. Insights Imaging. 2010;1:42–5, http://dx.doi.org/10.1007/s13244-010-0025-8.
33. Martí-Bonmatí L, Alberich-Bayarri Á, Alberich LC, Jiménez A. Imaging biomarkers in oncology. In: Neri E, Erba PA, editors. Multimodality imaging and intervention in oncology. Cham: Springer; 2023. p. 551–71, http://dx.doi.org/10.1007/978-3-031-28524-0_22.
34. Vera-Vera JF, Roldán-Nofuentes JA. A robust alternating least squares K-means clustering approach for times series using dynamic time warping dissimilarities. Math Biosci Eng. 2024;21:3631–51, http://dx.doi.org/10.3934/mbe.2024160.